PHYSICAL REVIEW C **69**, 051301(R) (2004)

Systematics of the bimodal isoscalar giant dipole resonance

M. Uchida,[1,*] H. Sakaguchi,[1] M. Itoh,[1,†] M. Yosoi,[1] T. Kawabata,[1,‡] Y. Yasuda,[1] H. Takeda,[1] T. Murakami,[1] S. Terashima,[1] S. Kishi,[1] U. Garg,[2] P. Boutachkov,[2] M. Hedden,[2] B. Kharraja,[2] M. Koss,[2] B. K. Nayak,[2] S. Zhu,[2] M. Fujiwara,[3,4] H. Fujimura,[3] H. P. Yoshida,[3] K. Hara,[3] H. Akimune,[5] and M. N. Harakeh[6]

[1]*Department of Physics, Kyoto University, Kyoto 606-8502, Japan*

[2]*Physics Department, University of Notre Dame, Notre Dame, Indiana 46556, USA*

[3]*Research Center for Nuclear Physics, Osaka University, Osaka 567-0047, Japan*

[4]*Advanced Science Research Center, Japan Atomic Energy Research Institute, Tokai 319-1195, Japan*

[5]*Department of Physics, Konan University, Kobe 658-8501, Japan*

[6]*Kernfysisch Versneller Instituut, 9747 AA Groningen, The Netherlands*

(Received 21 January 2004; published 17 May 2004)

The systematic behavior of the isoscalar giant dipole resonance (ISGDR) in ^{90}Zr, ^{116}Sn, ^{144}Sm, and ^{208}Pb is studied with inelastic α scattering at $E_\alpha = 386$ MeV. Multipole-decomposition analysis is applied to extract the excitation strengths of giant resonances from the (α, α') differential cross sections at $\theta_{\rm lab} = 0.64° - 13.5°$. The bimodal structure of the ISGDR is discussed and compared with recent theoretical results from Hartree-Fock+random-phase-approximation calculations.

DOI: 10.1103/PhysRevC.69.051301 PACS number(s): 24.30.Cz, 21.65.+f, 24.50.+g

The isoscalar giant dipole resonance (ISGDR) has been studied for more than 20 years because of its importance in determining the incompressibility of nuclear matter, as is the case for the isoscalar giant monopole resonance (ISGMR). This subject remains one of the active fields in nuclear-physics research because of continuing developments in experimental techniques as well as theoretical calculations. Indications of the excitation of the ISGDR were reported as early as in the 1980s [1–3], soon after a theoretical description for this mode was reported by Harakeh and Dieperink [4,5]. However, the first direct evidence for this mode was provided by Davis *et al.* in 1997 [6]. They demonstrated that in 200 MeV inelastic α scattering near 0°, the giant resonance bump at $3\hbar\omega$ excitation energy could be separated into two components, the ISGDR and the high energy octupole resonance (HEOR), by using the difference of spectra (DOS) method [7]. Further evidence for the ISGDR was obtained by Clark *et al.* from 240 MeV inelastic α-scattering measurements on ^{90}Zr, ^{116}Sn, ^{144}Sm, and ^{208}Pb [8], using a multipole-decomposition analysis (MDA).

Prior to our measurements, the ISGDR data presented a problem in that the experimental centroids of excitation energy of the ISGDR were significantly different from those obtained from the Hartree-Fock plus random-phase-approximation (HF+RPA) calculations. For example, the centroid of the ISGDR in ^{208}Pb was reported by Clark *et al.* [8] to be located at 19.9 ± 0.8 MeV. This low value was in disagreement with the theoretical values predicted at $E_x > 22$ MeV [10–16]. Also, the ISGDR energies in Ref. [8] and the known ISGMR energies [9] led to values of the incompressibility of the infinite nuclear matter that are different from each other by as much as 40%. The low values for the centroids reported by Clark *et al.* [8] now appear to have resulted from their background-subtraction procedure which rendered the ISGDR strength zero at $E_x > 24$ MeV. In our recent paper [17], this discrepancy was resolved for ^{208}Pb by using the MDA without any background subtraction in the analysis thanks to clean spectra obtained at extremely forward angles, including 0°.

An interesting aspect of the ISGDR strengths in ^{208}Pb is a bimodal distribution. The first experimental trial to extract the low-energy (LE) component of the ISGDR was performed by Clark *et al.* [8]. The low-energy $L=1$ strength has been predicted also in calculations that correctly account for the spurious 1^- state [10–12,14–16]. This component has been suggested to be related to surface oscillations or the toroidal modes [13]. A reliable experimental extraction of this LE ISGDR strength over a wide range of nuclei is important to confirm the theoretical prediction. However, it is very difficult to experimentally disentangle the LE ISGDR component from other modes of giant resonances by using simple analysis techniques such as the DOS method [6], because there are many modes of giant resonances such as ISGMR, isoscalar giant quadrupole resonance (ISGQR), low-energy octupole resonance (LEOR), and isovector giant dipole resonance (IVGDR) overlapping in the same excitation-energy region. The multipole decomposition analysis would appear to be the most suitable and effective approach to distinguish the various giant-resonance modes. In this article, we report results on the systematic behavior of the bimodal isoscalar giant dipole resonance studied via the ^{90}Zr, ^{116}Sn, ^{144}Sm, and ^{208}Pb(α, α') reactions.

The experiments were performed at the Research Center for Nuclear Physics (RCNP), Osaka University, using inelastic α scattering at $E_\alpha = 386$ MeV and at extremely forward angles, including 0°. Self-supporting targets of ^{90}Zr, ^{116}Sn,

*Present address: Research Center for Nuclear Physics, Osaka University, Osaka 567-0047, Japan.

†Present address: Research Center for Nuclear Physics, Osaka University, Osaka 567-0047, Japan.

‡Present address: Center for Nuclear Study (CNS), Graduate School of Science, University of Tokyo, Wako 351-0198, Japan.

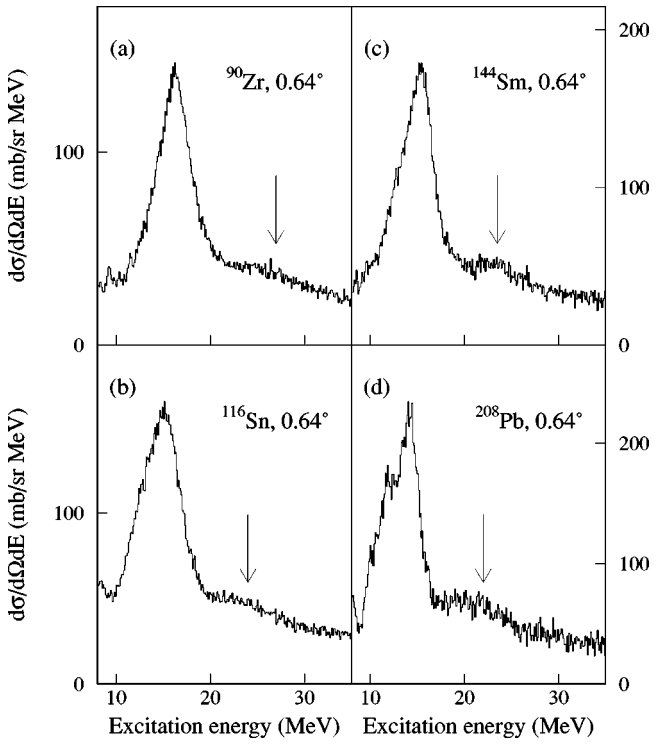

FIG. 1. Excitation energy spectra for ^{90}Zr, ^{116}Sn, ^{144}Sm, and ^{208}Pb at θ=0.64°. The arrows indicate the locations of the HE ISGDR. Note that the ^{144}Sm(α,α') spectrum from our previous work [21] is also included.

and ^{208}Pb were bombarded with a 386 MeV ^{4}He^{2+} beam from the RCNP ring cyclotron. Inelastically scattered particles were momentum analyzed with the high-resolution magnetic spectrometer Grand Raiden [18]. The focal-plane detection system consisted of two multiwire drift chambers (MWDC's) [19] and two plastic scintillation counters. Details of the experimental setup and data-analysis procedures are described in Refs. [17,20,21]. The energy spectra for each nucleus, virtually free from instrumental background, have been obtained in the range of $8 \leqslant E_x \leqslant 32$ MeV at a number of scattering angles between $0° < \theta < 13.5°$. The energy scale was calibrated using the discrete levels of ^{12}C (g.s., 4.439, 7.654, and 9.641 MeV states) in elastic and inelastic α-scattering.

Figure 1 shows the excitation energy spectra for ^{90}Zr, ^{116}Sn, ^{144}Sm, and ^{208}Pb at θ=0.64°. Broad bumps are clearly recognized at $E_x \sim 15$ MeV for all target nuclei. These bumps are mainly due to the ISGMR excitation. The peak positions of the bumps shift to lower excitation energy with increasing mass number of the target nucleus, which is consistent with the empirical mass dependence of the ISGMR [9]. The high-energy components of the ISGDR are expected in the energy region between 20 and 30 MeV. The bumps corresponding to the HE ISGDR are visible at the high-energy tail of the main bump, especially in ^{144}Sm and ^{208}Pb. The ISGQR and the IVGDR overlap in the region of ISGMR, and the HEOR coexists with the ISGDR. This experimental situation makes the extraction of individual giant resonance components difficult with simple peak-fitting methods.

TABLE I. Parametrizations for the density-dependent effective α-nucleon interaction.

Target	V (MeV)	α_V (fm^2)	β_V (fm^2)	W (MeV)	α_W (fm^2)	α_W (fm^2)
^{90}Zr	33.50	3.62	−1.9	13.21	4.55	−1.9
^{116}Sn	29.70	3.82	−1.9	14.82	4.15	−1.9
^{208}Pb	29.80	4.03	−1.9	16.97	4.17	−1.9

The angular distributions of the differential cross sections were obtained for each nucleus by sorting excitation-energy spectra in terms of scattering angles. Multipole decomposition analysis [22] was applied to extract the excitation strengths of the giant resonances in ^{90}Zr, ^{116}Sn and ^{208}Pb. Diffraction patterns of differential cross sections are empirically characterized in terms of the transferred J^π values. Thus, it is possible to reproduce experimental angular distributions at any excitation-energy region by a superposition of the calculated distorted-wave Born approximation (DWBA) cross sections for different sets of J^π values. Since in inelastic α scattering only the natural parity states are excited, the J^π values to be considered are sufficiently reduced, which is a great advantage over (e,e') and (p,p') reactions. In addi-

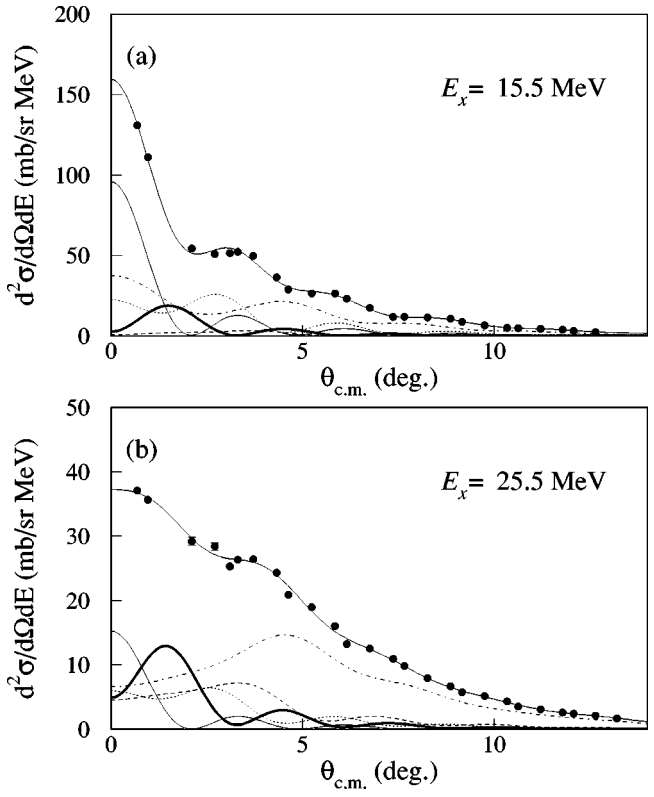

FIG. 2. Angular distributions of selected 1 MeV bins for the ^{116}Sn(α,α') reaction at 386 MeV. (a) Results for E_x=15.5 MeV, where the ISGMR is dominant. (b) Results for E_x=25.5 MeV, where the ISGDR is expected to be enhanced. The solid circles are the experimental data. The lines show contributions from L=0 (thin solid line), L=1 (thick solid line), L=2 (dotted line), L=3 (dashed line), and other higher components including IVGDR (dot-dashed line).

tion, the excitation of isovector resonances is greatly suppressed—the IVGDR is the only isovector resonance excited with any discernible strength in these measurements and is accounted for in the analysis.

The ISGMR and ISGDR strength distributions were obtained in the MDA. In this approach, the experimental angular distribution for each 1 MeV bin was fitted by using the following equation:

$$\left(\frac{d^2\sigma}{d\Omega dE}(\theta_{\mathrm{c.m.}},E_x)\right)^{\mathrm{expt}} = \sum_{L=0}^{L_{\max}} a_L(E_x)\left(\frac{d^2\sigma}{d\Omega dE}(\theta_{\mathrm{c.m.}},E_x)\right)_L^{\mathrm{calc}}, \tag{1}$$

where $(d^2\sigma/d\Omega dE)_L^{\mathrm{calc}}$ are the calculated DWBA cross sections corresponding to the full energy-weighted-sum-rule (EWSR) for a given multipole L. The fraction of the EWSR, $a_L(E_x)$, relates to the strength values of $S_L(E_x)$ as

$$S_L(E_x) = m_1 \frac{a_L(E_x)}{E_x}, \tag{2}$$

where m_1 is the full EWSR value defined as $m_1 = \Sigma E_x S_L(E_x)$.

The DWBA calculations were made in the framework of the single-folding model with a density-dependent effective α-N interaction [23] written as

$$V(|\mathbf{r}-\mathbf{r}'|,\rho_0(r')) = -V(1+\beta_V\rho_0^{2/3}(r'))e^{-|\mathbf{r}-\mathbf{r}'|^2/\alpha_V} - iW(1+\beta_W\rho_0^{2/3}(r'))e^{-|\mathbf{r}-\mathbf{r}'|^2/\alpha_W}. \tag{3}$$

All the parameterizations for the α-N interaction were determined by (α,α) reactions at the same incident energy, and are listed in Table I. The calculations were performed using the code ECIS95 [24], and the transition densities used in the calculations are described in Refs. [25,26]. The contributions from the IVGDR were subtracted by using the photoabsorption data [27] before performing the MDA, on the assumption that the EWSR value is exhausted.

Figure 2 shows the typical results of the MDA for the angular distributions of the ^{116}Sn(α,α') reaction at 386 MeV. In the fittings, we used the maximum number of the multipolarity as $L_{\max}=14$, resulting in a reduced χ^2 of $\chi^2/\nu \sim 1$, where ν is the number of degrees of freedom. In practice, the strengths and peak energies of the ISGMR and the ISGDR obtained from the MDA were stable in the case of $L_{\max} \geqslant 10$.

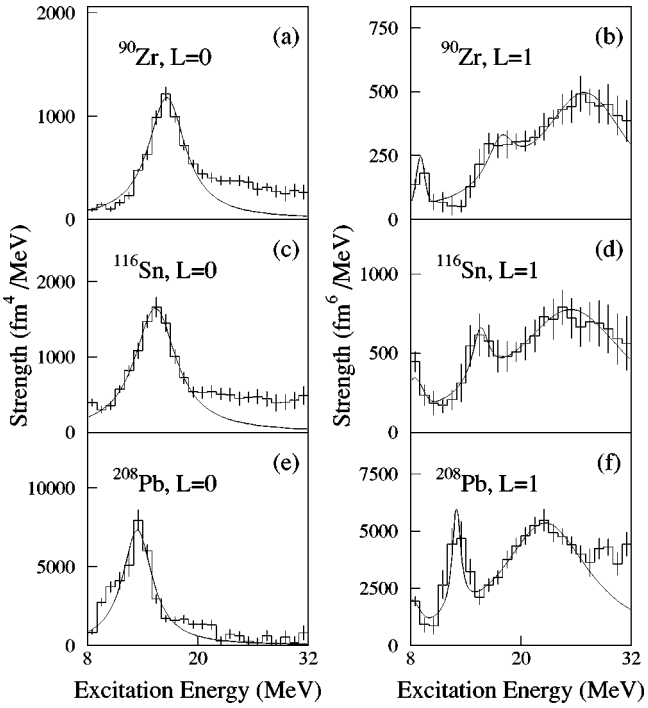

FIG. 3. Experimentally obtained strength distributions of the ISGMR and the ISGDR in ^{90}Zr, ^{116}Sn, and ^{208}Pb. The error bars are determined by changing the $E1$ strength within $\chi^{\mathrm{total}} \leqslant \chi^{\mathrm{total}}_{\min}+1$ in the MDA. In the case of the ISGMR, the results of fitting with a Breit-Wigner function are indicated. In the ISGDR's case, the results of fitting with two Breit-Wigner functions for the region of $E_x > 10$ MeV, and a Gaussian function for the peak at $E_x < 10$ MeV are included.

The strength distributions for the ISGMR and the ISGDR in ^{90}Zr, ^{116}Sn, and ^{208}Pb are shown in Fig. 3. The results obtained for the ISGMR ensure that the present analysis using the MDA is globally consistent with those obtained from the previously employed methods.

In the case of the ISGDR, the strength distributions have a clear two-peak structure in the region of $10 < E_x < 30$ MeV. This is expected in the theoretical calculations. An additional peak at $E_x < 10$ MeV is seen in each target. This might be part of the low-lying ISGDR strength observed previously by Poelhekken *et al.* [28] in their $(\alpha,\alpha'\gamma)$ study, or belong to the vortex mode states proposed in a recent (γ,γ') measurement in ^{208}Pb [29]; however, the present measurements can not distinguish between those

TABLE II. Peak energies, widths, and EWSR fractions for the ISGMAR and ISGDR. The errors in fitting the $L=0$ and $L=1$ strengths with the Breit-Wigner functions are included.

	ISGMR			LE ISGDR			HE ISGDR		
	E_{ISGMR} (MeV)	Γ (MeV)	EWSR (%)	E_{ISGDR} (MeV)	Γ (MeV)	EWSR (%)	E_{ISGDR} (MeV)	Γ (MeV)	EWSR (%)
^{90}Zr	16.6±0.1	4.9±0.2	101±3	17.8±0.5	3.7±1.2	7.9±2.9	26.9±0.7	12.0±1.5	67±8
^{116}Sn	15.4±0.1	5.5±0.3	95±4	15.6±0.5	2.3±1.0	4.9±2.2	25.4±0.5	15.7±2.3	68±9
^{144}Sm [21]	$15.3^{+0.11}_{-0.12}$	$3.70^{+0.12}_{-0.63}$	84^{+4}_{-25}	14.2±0.2	4.8±0.8	23^{+4}_{-10}	$25.0^{+1.7}_{-0.3}$	19.9±1.4	91^{+25}_{-17}
^{208}Pb	13.4±0.2	4.0±0.4	104±9	13.0±0.1	1.1±0.4	7.0±0.4	22.7±0.2	11.9±0.4	111±6

modes. It should be noted that the absolute value for the ISGDR strength in ^{208}Pb is larger by a factor of 3 than that described in our previous paper [17], because the definition of m_1 in Eq. (2) is different in our present paper according to the formula given in Ref. [26]; in Ref. [17], the formula used was taken from Ref. [5].

The high-lying tails of the $L=1$ component, which are typically observed in ^{208}Pb at $E_x > 28$ MeV, are partly due to the physical continuum with a characteristic $L=1$ transfer, for example, from direct knock-out processes of $(\alpha, \alpha' p)$ and $(\alpha, \alpha' n)$. This is a limitation of the MDA in that the L transfer from the resonance and quasifree parts cannot be distinguished. In recent coincidence experiments at KVI and at RCNP, protons emitted from the ISGDR in ^{208}Pb have been measured at backward angles using solid-state detector arrays in coincidence with inelastically scattered α particles. It was found that the contribution from the physical continuum was reduced thanks to the kinematical suppression, and the resonance parts of interest were greatly enhanced [31,32]. Although the obtained EWSR fractions and the widths derived from the MDA will be affected by the treatment of the physical continuum, the peak position for the ISGDR in ^{208}Pb remains consistent in both the singles and coincidence measurements.

Table II summarizes the experimental results for peak energies, widths, and EWSR fractions for the ISGMR and ISGDR. The EWSR fractions are derived by integrating the extracted strengths in the energy region of $8 < E_x < 33$ MeV. The results for the ISGDR are illustrated in Fig. 4. The peak energies of the ISGDR are compared with the theoretical calculations by Colò *et al.*, and found to deviate from the $133A^{-1/3}$ curve for ^{90}Zr and ^{116}Sn. This result suggests the possibility that the strengths of the ISGDR for lighter nuclei are fragmented at high-excitation energies of $E_x > 32$ MeV. The lower EWSR fraction values for ^{90}Zr and ^{116}Sn would support this possibility. In fact, Colò *et al.* suggest the existence of fragmented $L=1$ strengths in ^{90}Zr and ^{116}Sn at $E_x > 32$ MeV. In addition, Colò has shown that the centroid of the calculated ISGDR strength comes down by ~ 1 MeV when the effects of the continuum and the $2p$-$2h$ couplings are taken into account [30], leading to an incompressibility of infinite nuclear matter, $K_{nm}=215$ MeV, in ^{208}Pb. The K_{nm} value obtained in the analysis of ^{144}Sm is found to be $205 \leqslant K_{nm} \leqslant 240$ MeV in Ref. [20], which is consistent with the present analysis in ^{208}Pb. It is noteworthy that the experimental results for the peak energies of the LE and HE components are in global qualitative agreement with the theoretical calculations.

In conclusion, we have reported the strength distributions of the ISGDR in ^{90}Zr, ^{116}Sn, ^{144}Sm, and ^{208}Pb obtained from the (α, α') experiments at $E_\alpha = 386$ MeV. The bimodal structures of the ISGDR have been found, and discussed in relation to the recent theoretical results. The peak energies of the ISGDR in ^{144}Sm and ^{208}Pb agree with the theoretical results

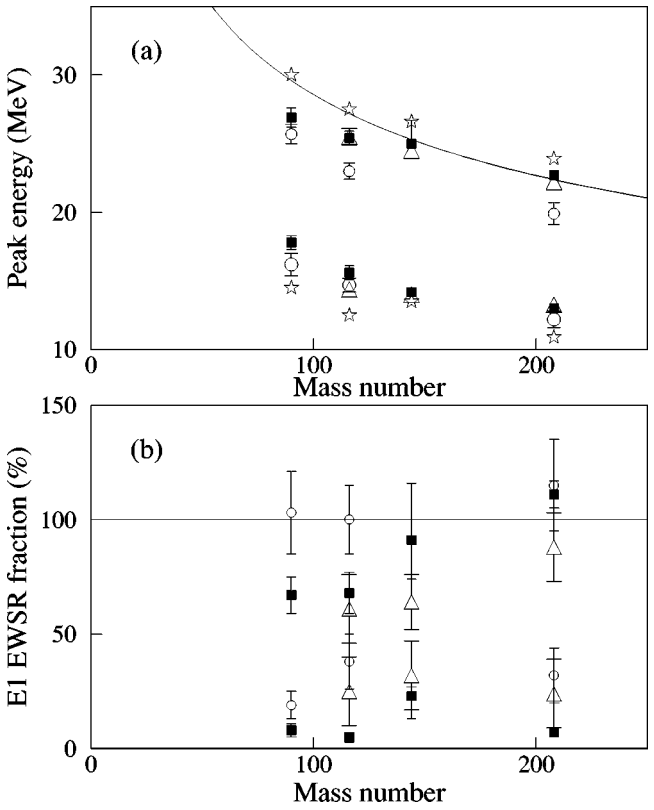

FIG. 4. Systematics of (a) the ISGDR peak energy and (b) the $E1$ EWSR fraction as a function of mass number. The solid squares, open circles, open triangles and stars are the results from the present work, from Clark *et al.* [8], current results from Youngblood *et al.* [33], and the theoretical calculation by Colò *et al.* [11], respectively. The error bars quoted for the EWSR fractions are only statistical. The systematic errors for the HE component of the ISGDR are estimated to be large due to the $L=1$ contributions from the continuum, especially at high excitation energies ($28 < E_x < 32$ MeV), which might result from processes unaccounted for in our analysis (for example, quasifree scattering and second-order effects). A $133A^{-1/3}$ curve, adjusted to pass through the ^{144}Sm and ^{208}Pb data points, is shown to guide the eye.

with the incompressibility of $K_{nm} \sim 215$ MeV. In ^{90}Zr and ^{116}Sn, small disagreements still remain between the experimental and theoretical results for the ISGDR peak energies. It should be noted here that the recent results for the ISGDR reported by Youngblood *et al.* [33] are very close to our present results. Experimentally, further work is required to extract reliable ISGDR strengths at high excitation energies in lighter nuclei (^{90}Zr, ^{116}Sn) by means of (α, α') singles as well as $(\alpha, \alpha' p)$ coincidence reactions.

This work was supported in part by the U.S.-Japan Cooperative Science Program of the JSPS, the U.S. National Science Foundation (Grant Nos. INT-9910015 and No. PHY-9901133), and the University of Notre Dame.

[1] H. P. Morsch, M. Rogge, P. Turek, and C. Mayer-Böricke, Phys. Rev. Lett. **45**, 337 (1980).
[2] C. Djalali, N. Marty, M. Morlet, and A. Willis, Nucl. Phys. **A380**, 42 (1982).
[3] G. S. Adams, T. A. Carey, J. B. McClelland, J. M. Moss, S. J. Seestrom-Morris, and D. Cook, Phys. Rev. C **33**, 2054 (1986).
[4] M. N. Harakeh, Phys. Lett. **90B**, 13 (1980).
[5] M. N. Harakeh and A. E. L. Dieperink, Phys. Rev. C **23**, 2329 (1981).
[6] B. F. Davis *et al.*, Phys. Rev. Lett. **79**, 609 (1997).
[7] S. Brandenberg *et al.*, Nucl. Phys. **A466**, 29 (1987).
[8] H. L. Clark, Y.-W. Lui, and D. H. Youngblood, Phys. Rev. C **63**, 031301(R) (2001).
[9] D. H. Youngblood, H. L. Clark, and Y.-W. Lui, Phys. Rev. Lett. **82**, 691 (1999).
[10] I. Hamamoto and H. Sagawa, Phys. Rev. C **66**, 044315 (2002).
[11] G. Coló, N. Van Giai, P. F. Bortignon, and M. R. Quaglia, Phys. Lett. B **485**, 362 (2000).
[12] J. Piekarewicz, Phys. Rev. C **62**, 051304(R) (2000); **64**, 024307 (2001).
[13] D. Vretenar, N. Paar, P. Ring, and T. Nikšić, Phys. Rev. C **65**, 021301(R) (2002).
[14] S. Shlomo and A. I. Sanzhur, Phys. Rev. C **65**, 044310 (2002).
[15] M. L. Gorelik and M. H. Urin, Phys. Rev. C **64**, 047301 (2001).
[16] V. I. Abrosimov, A. Dellafiore, and F. Matera, Nucl. Phys. **A697**, 748 (2002).
[17] M. Uchida *et al.*, Phys. Lett. B **557**, 12 (2003).
[18] M. Fujiwara *et al.*, Nucl. Instrum. Methods Phys. Res. A **422**, 484 (1999).
[19] T. Noro *et al.*, RCNP Annual Report, 1991, p. 177.
[20] M. Itoh *et al.*, Phys. Lett. B **549**, 58 (2002).
[21] M. Itoh *et al.*, Phys. Rev. C **68**, 064602 (2003).
[22] B. Bonin *et al.*, Nucl. Phys. **A430**, 349 (1984).
[23] A. Kolomiets, O. Pochivalov, and S. Shlomo, Phys. Rev. C **61**, 034312 (2000).
[24] J. Raynal, Program ECIS95 NEA 0850/14, 1996.
[25] G. R. Satchler, Nucl. Phys. **A472**, 215 (1987).
[26] M. N. Harakeh and A. van der Woude, *Giant Resonances: Fundamental High-Frequency Modes of Nuclear Excitation* (Oxford University Press, Oxford, 2001).
[27] S. S. Dietrich and B. L. Berman, At. Data Nucl. Data Tables **38**, 199 (1998).
[28] T. D. Poelhekken, S. K. B. Hesmondhalgh, H. J. Hofmann, A. van der Woude, and M. N. Harakeh, Phys. Lett. B **278**, 423 (1992).
[29] N. Ryezayeva, T. Hartmann, Y. Kalmykov, H. Lenske, P. von Neumann-Cosel, V. Yu. Ponomarev, A. Richter, A. Shevchenko, S. Volz, and J. Wambach, Phys. Rev. Lett. **89**, 272502 (2002).
[30] G. Coló, N. Van Giai, P. F. Bortignon, and M. R. Quaglia, RIKEN Rev. **23**, 39 (1999); (private communication).
[31] M. Hunyadi *et al.*, Phys. Lett. B **576**, 253 (2003).
[32] U. Garg, Nucl. Phys. **A731**, 3 (2004).
[33] D. H. Youngblood, Y.-W. Lui, H. L. Clark, B. John, Y. Tokimoto, and X. Chen, Phys. Rev. C **69**, 034315 (2004).